Pd/C Catalysts Prepared by Controlled Adsorption of Pd(II) Species on SX PLUS Carbon in the Aqueous Phase

Aurore Deffernez, Sophie Hermans, and Michel Devillers*

Université Catholique de Louvain, Unité de Chimie des Matériaux Inorganiques et Organiques, Place Louis Pasteur1/3, B-1348 Louvain-la-Neuve, Belgium

Received: January 17, 2007; In Final Form: April 18, 2007

Pd/C catalysts were prepared on SX PLUS activated carbon by a controlled adsorption method in which the interactions between the Pd precursor and the carbonaceous support in aqueous solution were optimized. This strategy involved (i) determining the surface charge state of the carbon support as a function of the pH, (ii) establishing adsorption curves for Pd on C to identify the pH windows where maximum adsorption occurs, and (iii) determining the distribution of Pd(II) species in solution from the stability constants of the various compounds involving the ligands H_2O, OH^-, and/or Cl^-. It was found that the charge of metal species present in solution, which depends on the pH, influences markedly the adsorption of Pd on carbon. The actual catalysts were then prepared by keeping the pH of the impregnating Pd solution within the optimal adsorption range throughout all synthetic steps, followed by chemical or thermal activation. This optimized preparation method led to highly efficient catalysts for the selective oxidation of glyoxal into glyoxalic acid, with activities superior to that of comparable monometallic materials (prepared by other methods or commercial manufacturing) and equivalent to that of bimetallic (promoted) catalysts. The Pd/C catalysts were characterized by XPS, SEM, TEM, and CO chemisorption, and it was found that the catalytic activity could be correlated to high Pd dispersion in the form of very small particles homogeneously dispersed on the support and to an important degree of Pd reduction.

1. Introduction

Carbon-supported palladium catalysts are used for a great number of industrial processes among which are hydrogenations and oxidations in the liquid phase.[1] Selective oxidations are related to the manufacturing of organic fine chemicals and the production of intermediates for the food, cosmetic, and pharmaceutical industries.[2−6] However, despite a large number of patents and papers dealing with the preparation of Pd/C catalysts,[7] for example, using deposition−precipitation,[8] incipient wetness,[9] adsorption with or without in situ chemical reduction,[10−14] or ion exchange[10] techniques, new developments remain empirical in character, meaning that the resulting chemical and physical state of the surface structures is complex and inhomogeneous. Moreover, the surface of the activated carbons (the most commonly used carbonaceous support material) presents different types of functional groups containing heteroatoms (O, N, and S),[15] in varying amounts, which can be divided into acidic, neutral, and basic functions. This influences their surface characteristics and adsorption behavior. In particular, the carbon surface can be either positively or negatively charged in aqueous solution, below or above a characteristic pH value,[16] usually called the point of zero charge (PZC). It should be noted, however, that a strict definition for the PZC is related to the total absence of positive or negative charges at the surface.[17] Another possibility exists to reach a global net charge equal to zero: the presence of an equal number of positive and negative charges at the surface, which is the definition of the isoelectric point (IEP).[17] For simple inorganic oxides, in which acido−basicity is related to the presence of surface M−OH groups, it is relatively easy to distinguish between these two notions because the coexistence of positively and negatively charged groups is governed by the difference in the pK_a values of the two acid−base couples involved (MOH_2^+/MOH and MOH/MO^-). For active carbons, due to the presence of a large number of surface functions of varying nature (and thus varying acido−basic character), confusion exists between the two parameters: most authors claim to measure either one or the other or even associate them.[18,19]

It seems obvious that the preparation of Pd/C catalysts in aqueous solution must take these physicochemical aspects into consideration to obtain the desired characteristics for the synthesized materials, such as highly dispersed metallic particles. It is well-established that the adsorption capacity of activated carbons in the aqueous phase depends on their surface area, pore volume, and pore size distribution and is strongly influenced by the presence of surface functional groups, which influence the PZC and IEP values. At the pH corresponding to the PZC, the net overall surface charge would be zero; at pH > pH_{PZC}, the negatively charged carbon surface attracts cations from solutions, while at pH < pH_{PZC}, it attracts anions. This kind of methodology was used by Regalbuto's group[16] to obtain highly loaded, highly dispersed Pt/carbon materials for applications as fuel cell electrocatalysts. Their results suggested that metal uptake attains a maximum with respect to pH for a given metal precursor and carbon PZC (i.e., the highest PZC carbons adsorb the most $[PtCl_6]^{2-}$ anions and the least $[Pt(NH_3)_4]^{2+}$ cations, while the lowest PZC carbon adsorb the least anions and the most cations, implying an electrostatic mechanism of adsorption). Therefore, it is important to know, on the one hand, the evolution of the carbon surface charge as a function of the

* To whom correspondence should be addressed. Tel.: +32 10 47 28 27; fax: +32 10 47 23 30; e-mail: devillers@chim.ucl.ac.be.

10.1021/jp070402u CCC: $37.00
Published on Web 06/02/2007

pH and, on the other hand, the influence of the charge of the metallic species present in solution on their adsorption behavior.

The reaction considered in this study is the liquid-phase oxidation of glyoxal into glyoxalic acid. This targeted acid is of interest in fine chemicals synthesis, for example, in the preparation of drug modifiers, cosmetics, perfumes, and agricultural products[20] and, in particular, for the synthesis of penicillin and vanillin.[21] It is also used in condensation reactions with phenols to give sophisticated molecules, in peptide synthesis, and in histochemical fluorescence for cell analysis. Finally, this acid and its derivatives are extremely useful in organic synthesis,[22] in reactions with amines, amides, or sulfonamides to give α-amino acids and α-alkoxy esters.[23] Various processes are known for the preparation of glyoxalic acid, and not all of them start from glyoxal.[24−28] However, each of these methods presents some serious unresolved disadvantages, meaning that glyoxalic acid is an expensive fine chemical. It is routinely prepared in the industry by stoichiometric nitric acid oxidation of glyoxal. In spite of the yield reaching up to 75%, a large amount of nitrogen oxides (NO_x), seriously harmful to the environment, are being generated in the process. The other possibilities are not commercial: biocatalytic methods[24−26] are limited by the difficulty in separating glyoxalic acid from the reaction mixture, while electrochemical oxidation of glyoxal on platinum anodes[27] or the simultaneous anodic oxidation of glyoxal and cathodic reduction of oxalic acid[28] are restricted by the complexity in eliminating completely the remaining glyoxal from the solution and in obtaining highly concentrated products. To overcome these problems, a heterogeneous catalytic process in aqueous solution, using air as oxidant, thus producing a minimum of waste and offering the possibility of catalyst recycling, would be ideal. In 1992, Gallezot et al. reported that Pt and Pd carbon-supported catalysts were suitable for glyoxal oxidation[29] and that they gave better results than Ru/C or Rh/C. Since then, promoted M−Pd/C catalysts (M = Bi, Pb, Ru, or Au) have been developed in our laboratory and have been shown to be more active and selective than the monometallic formulations.[30−34] However, the preparation methods of these carbon-supported catalysts have never been optimized. Therefore, it seemed important to improve the surface properties of monometallic catalysts to improve their catalytic properties and, later, to optimize the bimetallic materials.

In this work, we have optimized the Pd(5 wt %)/C catalyst preparation method by maximizing the interactions between the Pd precursor and the carbonaceous support in aqueous solution. This includes the following steps: first, the activated carbon support was characterized by determination of its PZC and its IEP; second, the influence of the charge of the palladium(II) species present in solution on the adsorption behavior was studied; finally, these adsorbed Pd samples were reduced to metallic Pd/C catalysts, and different activation methods were compared. All prepared catalysts were compared on the basis of the yield and selectivity in glyoxalic acid obtained in glyoxal oxidation carried out in the aqueous phase. The selectivity is an important parameter because a variety of byproducts might be formed in this reaction: glycolic acid by Cannizzaro dismutation and oxalic and formic acids by over-oxidation, as described previously[32−34] and shown in Figure 1. A preliminary account of parts of this work has already been reported elsewhere.[35]

2. Experimental Procedures

2.1. Starting Materials. An activated carbon, carbon SX PLUS supplied by NORIT (abbreviated as C in this paper,

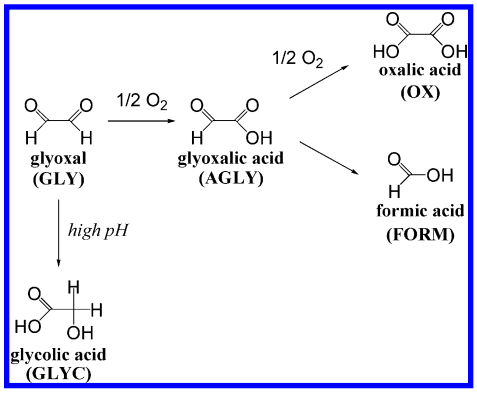

Figure 1. Catalytic oxidation of glyoxal: possible byproducts.

$S_{BET} \approx 900$ m^2 g^{-1}, particle size = 50−100 μm, total acidity = 32.0 mmol/100 g) was used as a support. A batch of this support was submitted to an oxidation treatment, as described previously,[36] by refluxing for 24 h in 2.5 mol/L HNO_3, to increase the number of oxygenated surface functions (functionalized carbon (abbreviated as C_f in this paper), $S_{BET} \approx 750$ m^2 g^{-1} and total acidity = 325.6 mmol/100 g). Two palladium precursors were used: palladium(II) acetate ($Pd(OAc)_2$, Aldrich, 98%) and palladium(II) chloride ($PdCl_2$, Aldrich, 99.9+ %).

2.2. Determination of PZC and IEP. The PZC (pH at which the net surface charge is zero) of the carbon support was determined by two different experimental procedures: the so-called mass titration method[37] and a modified version of the method proposed by Park and Regalbuto.[38] In the mass titration method, aqueous suspensions of initial fixed pH values were prepared with increasing mass percentages of carbon. After 24 h stirring, the pH of the suspensions was determined, and the PZC was the pH value obtained as the plateau of the measured pH versus mass curve (the corresponding pH value being independent of the initial pH of the aqueous suspension). The second method involved bringing 1 g of carbon in contact with 10 mL of water at a fixed pH and measuring the resulting pH after 24 h by using a pH electrode. This operation was repeated over a wide range of initial pH values (1−13). The PZC is the plateau obtained when plotting the measured pH versus the initial fixed pH.

The IEP (point of zero net mobility) was determined by electrophoretic mobility measurements using a Laser Zee Meter 500 apparatus (Pen-Kem Inc.), with 10^{-3} mol/L KNO_3 as the supporting (indifferent) electrolyte. A limitation of this method is that the measurements can be realized only for pH values between 3 and 10. The carbon suspension in KNO_3 solution was left to rest for 24 h, and the experiments were performed with only the supernatant to minimize aggregation effects (i.e., the settled particles were discarded by decantation before the measurements). The IEP value corresponds to the intersection of the curve of electrophoretic mobility versus pH with the abscissa axis.

2.3. Establishment of Adsorption Curves. An aqueous solution of given (calculated in the following) palladium concentration at fixed pH was added to an aqueous suspension of 0.238 g of carbon pre-conditioned at the same pH value to obtain a final volume of 100 mL. After 24 h stirring, the adsorption filtrate containing the non-adsorbed Pd was analyzed by atomic absorption spectrometry, and the amount of Pd adsorbed on the support was deduced by subtraction. The amount of metal introduced in solution was calculated by considering a monolayer of metallic precursor molecules on the SX PLUS carbon surface (macro- and mesopores included, $S_{BJH} = 245$ m^2/g for the SX PLUS carbon) and neglecting the

area developed by the micropores. In the case of the functionalized carbon, the same palladium charge was used for comparison, even though the surface developed by the macro- and mesopores of this modified carbon sample was lower (S_{BJH} = 160 m^2/g). This means that, in the case of $Pd(OAc)_2$, a mass of 0.053 g was taken, while 0.042 g was used in the case of $PdCl_2$. Consequently, the Pd/C sample produced in the case of 100% adsorption corresponds to a loading of Pd(9.52 wt %)/C. This turns down all possibilities of precipitation because we have verified, by calculation (using $10^{-2.35}$ as the K_s value[39]), that these experimental conditions do not lead to the formation of the $Pd(OH)_2$ species, for all pH values below 14. This experiment was repeated over the whole spectrum of pH values ranging from 1 to 14, at every step of 0.5 pH units.

Additional experiments were carried out to understand the role of ions such as Na^+ and Cl^- on the Pd dispersion. The adsorption of palladium acetate solubilized by nitric acid was investigated again, at four different fixed pH values, in the presence of sodium chloride. The amount of NaCl introduced was calculated so that it corresponded to twice the equivalent of sodium with respect to the amount of Na_2CO_3 added to fix the pH of the solution.

2.4. Catalysts Synthesis. The Pd(5 wt %)/C catalysts were synthesized by impregnation in aqueous solution. The carbon support (0.475 g) was suspended in distilled water (50 mL) at a fixed pH for 24 h. The metallic precursor (0.053 g for $Pd(OAc)_2$ or 0.042 g for $PdCl_2$) was dissolved in concentrated nitric or hydrochloric acid before the addition of distilled water to reach a volume of 50 mL. The pH of this solution was then adjusted to the selected value with Na_2CO_3 or NaOH. The suspension of carbon was added to the Pd solution and stirred for a further 24 h. The catalyst was activated in situ at 80 °C, after the addition of a base (NaOH) to reach a fixed pH (detailed in the Results), by chemical reduction with 1 mL of formalin (aqueous solution of formaldehyde 37 wt %). Finally, the activated catalyst was recuperated by filtration. When palladium chloride was used as the metallic precursor, or HCl as the solubilizing agent, the obtained catalyst was washed with warm distilled water several times to eliminate residual chlorine, and the final filtrate was tested for Cl^- with $AgNO_3$. Other activation methods were also used: either in situ reduction of the precursor salts with sodium borohydride ($NaBH_4$) in aqueous solution or thermal activation at 350 °C for 18 h under a flow of pure hydrogen (H_2) or nitrogen (N_2) in a tubular oven.

2.5. Catalytic Tests. All catalytic tests were performed, as described previously,[30,31] in a thermostatized double-walled glass reactor equipped with an automatic titration device (Stat Titrino 718 from Metrohm) to keep the pH constant at a value of 7.2 by the addition of a solution of 0.3 mol/L Na_2CO_3. The reaction conditions were fixed as follows: 400 mL of glyoxal (0.1 mol/L), temperature = 38 °C, 0.1 g of catalyst, duration = 20 h, stirring rate = 1000 rpm, air flow = 0.4 L/ min. The duration of the catalytic tests was fixed at 20 h because detailed kinetic studies of this reaction have shown that, with most catalysts, the maximum yield in glyoxalic acid is not yet attained after this period of time. This allows comparisons between different materials to be made, without the risk of underevaluating the activity if some glyoxalic acid was transformed further into oxalic acid as would be the case after this maximum.[32,33] All reaction filtrates were analyzed by atomic absorption spectrometry, but no metal leaching was found. The catalytic results, determined by HPLC (Thermo Separation Products chromatograph equipped with a Spectra System UV 6000LP detector) on an Aminex column (Biorad HPX-87H) with a sulfuric acid solution (0.005 mol/L) as eluent, are expressed in terms of yield in each different product (Y, %), corrected conversion (X^*, %) and corrected selectivity (S^*, %).[32−34] The corrected parameters do not take into account the production of glycolic acid, which depends only on the pH (see Figure 1). These parameters are defined as follows:

$$Y_{\text{product}} = C_{\text{product}}/C_{\text{GLY}}$$

where C is the concentration and product is AGLY, OX, GLYC, or FORM; see Figure 1 for abbreviations.

$$X^*_{\text{GLY}} = Y_{\text{AGLY}} + Y_{\text{OX}} + (Y_{\text{FORM}}/2)$$

$$S^*_{\text{AGLY}} = (Y_{\text{AGLY}}/X^*_{\text{GLY}})100$$

2.6. Physicochemical Characterization Techniques. The solid samples were characterized by X-ray photoelectron spectroscopy (XPS), scanning electron microscopy (SEM), transmission electron microscopy (TEM), and CO chemisorption.

XPS was performed on an SSI−-X probe (SSX-100/206) spectrometer from Fisons. The samples were adhered onto small troughs with double-sided adhesive tape and then placed on an insulating homemade ceramic carrousel with a nickel grid positioned 3 mm above the sample surface, to avoid differential charging effects. A floodgun set at 8 eV was also used for charge stabilization. The energy scale was calibrated by taking the Au $4f_{7/2}$ binding energy at 84 eV. The C_{1s} binding energy of contamination carbon set at 284.8 eV was used as internal standard value. The analysis of palladium was based on the Pd 3d photopeaks, and the following constraints were used for decomposition: intensity ratios $I(Pd\ 3d_{5/2})/I(Pd\ 3d_{3/2})$ fixed at 1.5, fwhm ratio = 1, $\Delta(Pd\ 3d_{5/2} - Pd\ 3d_{3/2}) = 5.26$ eV. Data treatment was performed with the CasaXPS program (Casa Software Ltd).

SEM analyses were performed on a field effect gun Digitan scanning electron microscope (DSM 982 Gemini from LEO). The powder samples were pressed onto conducting double-faced adhesive tape fixed onto 0.5 in. aluminum specimen stubs from Agar Scientific. The TEM images were acquired on a LEO 922 microscope, operating at a 200 kV accelerating voltage in bright field mode. The samples were deposited, from a suspension in hexane, on a holey carbon film supported on a copper grid (Agar Scientific) and allowed to dry in the air.

CO chemisorption measurements were carried out on an ASAP 2000 apparatus from Micromeritics. The samples (∼100 mg) were first submitted to pretreatment at 100 °C under He for 30 min followed by 10 min at 100 °C under hydrogen. The catalyst was then reduced during 2 h at 350 °C under H_2. The Pd dispersion was calculated by considering a surface Pd/CO stoichiometry equal to 1.

The quantification of Pd in solution for adsorption filtrates, catalyst synthesis filtrates, or catalytic test filtrates was determined by atomic absorption analysis, using a PerkinElmer 3110 spectrometer equipped with an air-acetylene flame atomizer. A calibration curve (from 1 to 10 mg/L) was realized with standard solutions obtained by dilution of a commercial palladium solution (1 g/L, Acros).

3. Results

3.1. Determination of Carbon PZC and IEP. Using the mass titration method, graphs showing the measured pH values of aqueous suspensions of carbon support, with increasing mass percentages of carbon in suspension, as a function of the mass

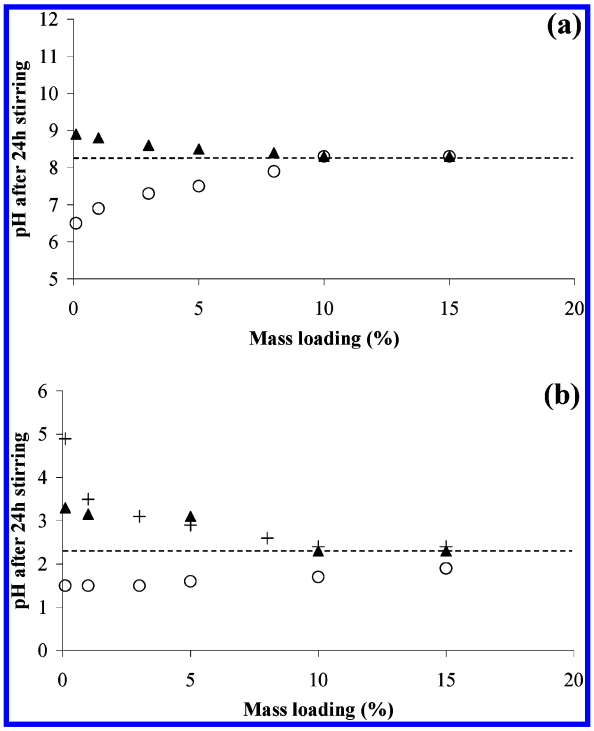

Figure 2. Determination of PZC by mass titration for (a) the activated carbon SX PLUS (▲ initial pH = 11.2 and ○ initial pH = 5.6) and (b) the functionalized carbon (+ initial pH = 7.7, ▲ initial pH = 3.4, and ○ initial pH = 1.5).

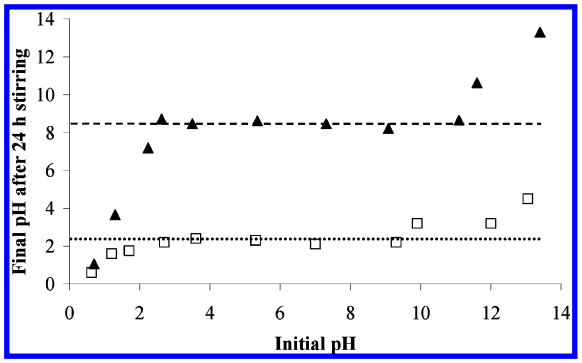

Figure 3. Determination of PZC by the method of Regalbuto and Park:[38] ▲ SX PLUS carbon, □ functionalized carbon, --- PZC of SX PLUS carbon, and ··· PZC of functionalized carbon.

of carbon, were established (Figure 2). The PZC values deduced from these graphs are, respectively, of 8.3 and 2.4 for the activated carbon SX PLUS (C) and the functionalized carbon (C_f). When using the method recommended by Park and Regalbuto[38] (slightly modified, see Experimental Procedures), the results obtained for SX PLUS (C) and functionalized (C_f) carbons are shown in Figure 3: the plateau corresponds to PZC values of 8.5 and 2.3, respectively.

The two plots leading to IEP determination for the two carbon samples are shown in Figure 4. In the case of SX PLUS carbon, the obtained value is approximately 3.5, while in the case of the functionalized carbon, a value lower than 2 can be extrapolated.

3.2. Establishment of Adsorption Curves. The pH range where maximum adsorption of Pd on the two carbon supports (C_{SXPLUS} (C) and functionalized carbon (C_f)) occurs has been determined for the two Pd precursors in aqueous solution and using either HNO_3 or HCl as a solubilizing agent. This means

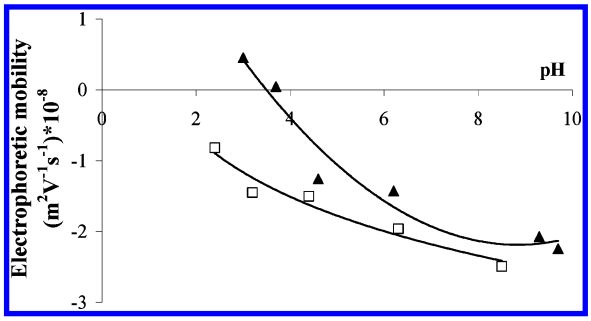

Figure 4. Determination of the IEP by electrophoretic mobility measurements: ▲ SX PLUS carbon and □ functionalized carbon.

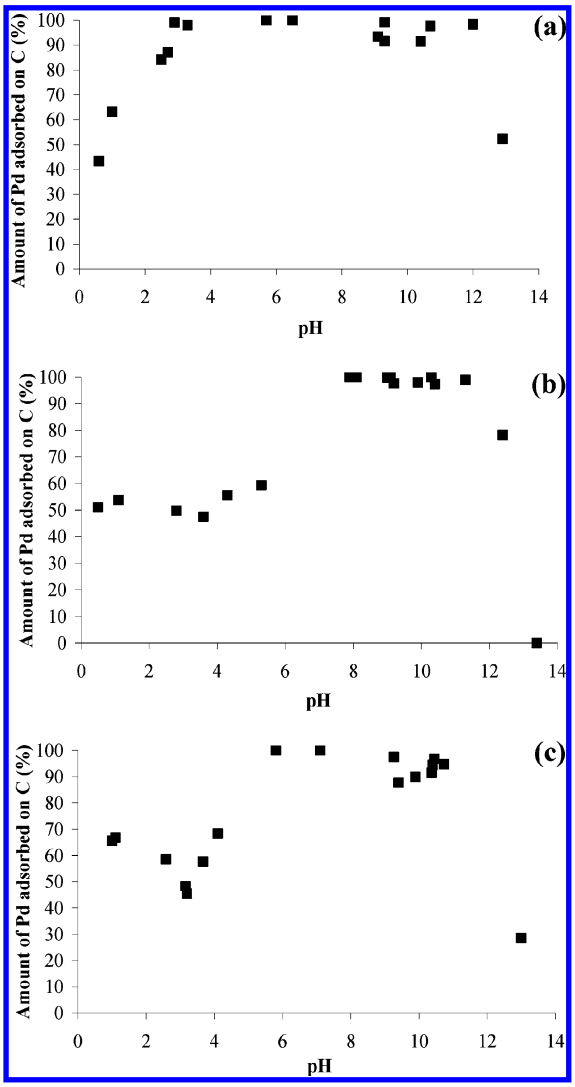

Figure 5. Adsorption curves, in aqueous solution, for the two Pd(II) precursors on carbon SX PLUS: (a) $PdCl_2 + HNO_3$, (b) $Pd(OAc)_2 + HCl$, and (c) $PdCl_2 + HCl$.

that eight different adsorption curves have been determined experimentally. As described previously,[35] the case of palladium acetate as a palladium precursor and nitric acid as a solubilizing agent gives a maximum adsorption range on C_{SXPLUS} that has been identified between pH 2.5 and 12.5. The experiment realized with Pd chloride solubilized with nitric acid gives a maximum adsorption window, on SX PLUS carbon, situated between pH 3 and 12 (Figure 5a). The window for maximum adsorption is further reduced, between pH 6 and 12, for the two cases corresponding to the use of HCl as a solubilizing

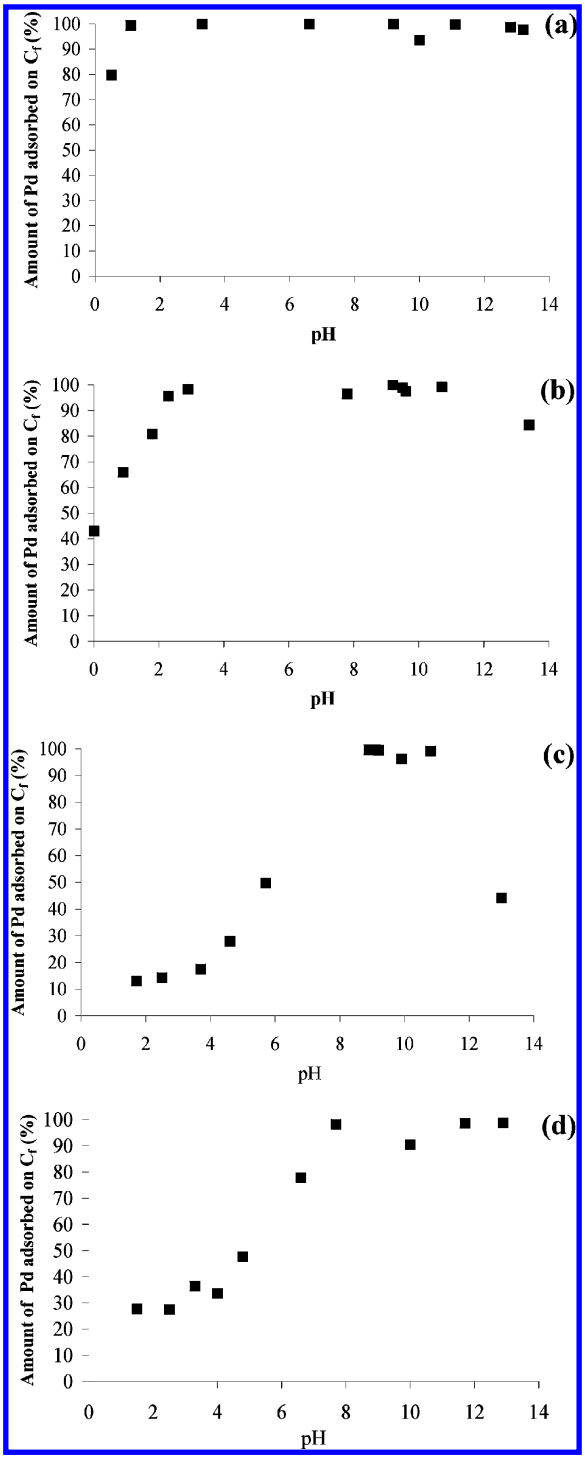

Figure 6. Adsorption curves, in aqueous solution, for the two Pd(II) precursors on functionalized carbon: (a) $Pd(OAc)_2 + HNO_3$, (b) $PdCl_2 + HNO_3$, (c) $Pd(OAc)_2 + HCl$, and (d) $PdCl_2 + HCl$.

agent, with both Pd precursors (Figure 5b,c). The four adsorption curves for the functionalized carbon seem to give the same pH windows as with C_{SXPLUS} but wider by at least one pH unit on each side in some cases (Figure 6). For example, the case of palladium acetate as a palladium precursor and nitric acid as a solubilizing agent gives a maximum adsorption range on functionalized carbon between pH 1 and 13.5 (Figure 6a) to compare with 2.5−12.5 on C_{SXPLUS}. Characterization by XPS of the solid samples prepared in the maximum adsorption range show that the Pd/C surface atomic intensity ratios are very

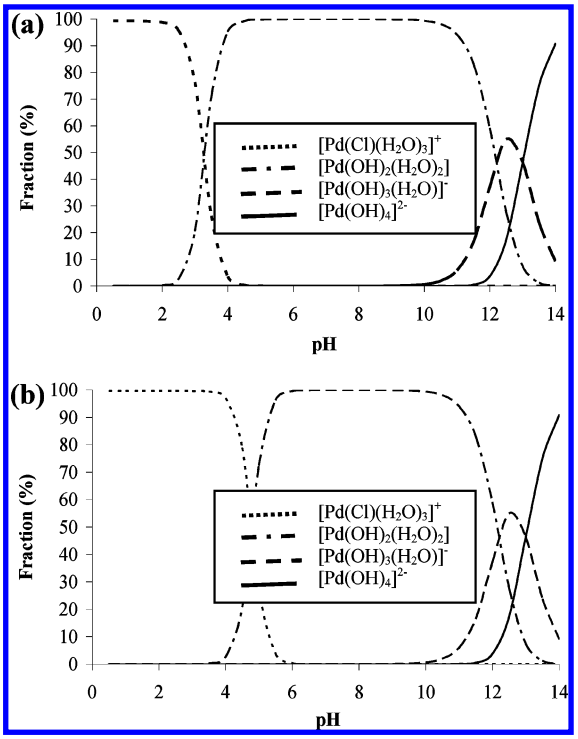

Figure 7. Pd(II) speciation diagrams as a function of pH for chlorinated species: (a) $PdCl_2 + HNO_3$ (pCl value of 2.93) and (b) $Pd(OAc)_2$ or $PdCl_2 + HCl$ (pCl value of 0.92).

high: 0.036−0.131 and 0.025−0.116 for the samples obtained with C_{SXPLUS} and functionalized carbon, respectively.

The results obtained in the presence of NaCl (adsorption of $Pd(OAc)_2$ solubilized by HNO_3) indicate that Na^+ and Cl^- ions play no role in Pd adsorption at three pH values (8.5, 9.6, and 10.7), for which 100% of Pd introduced is adsorbed on SX PLUS carbon, but they decrease this amount by a factor of 2 at a pH of 4.9.

3.3. Distribution of Pd Species in Solution. The distribution of Pd(II) species in solution was determined over the whole pH range from the stability constants,[40,41] by taking as a working hypothesis that $Pd(OAc)_2$ becomes $[Pd(H_2O)_4]^{2+}$ in acidic aqueous solution in the absence of chlorine, or becomes $[Pd(H_2O)_x(Cl)_{4-x}]^{(x-2)+}$ in chlorinated medium, and by calculating the actual chloride concentration from the amount of HCl added and/or the amount of Cl^- coming from the $PdCl_2$ precursor. This theoretical part must be connected with the experimental conditions used for the establishment of the adsorption curves and therefore with the synthesis conditions of the catalysts. Two chloride concentrations were considered, the first one corresponding to the use of $PdCl_2$ as a palladium precursor and HNO_3 to solubilize it, giving a pCl equal to 2.93, and the second one corresponding to the use of HCl to solubilize any of the two Pd precursors (giving the same actual chloride concentration), resulting in a pCl value of 0.92. Therefore, there is only one variable: the proton concentration (i.e., pH). Eqs 1−5 were used to establish the distribution curves shown in Figure 7. The speciation diagram for the chlorine-free case has already been reported in the preliminary paper.[35]

$$[Pd_{tot}] = [Pd^{2+}]\{1 + \sum_{n=1}^{4}(\beta_{OHn}[H^+]^{-n} + \beta_{Cln}[Cl^-]^n)\} \quad (1)$$

$$[[Pd(OH)_n(H_2O)_{4-n}]^{(2-n)+}] = \beta_{OHn}[Pd^{2+}][H^+]^{-n} \quad n = 0, 1, 2, 3, 4 \quad (2)$$

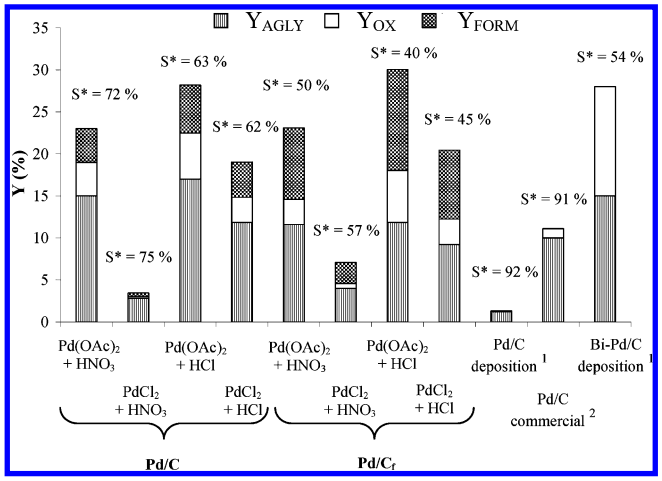

Figure 8. Comparison of catalytic results after 20 h for Pd(5 wt %)/C and Bi(5 wt %)-Pd(5 wt %)/C materials. C_f = functionalized carbon. Preparation conditions: $Pd(OAc)_2 + HNO_3$: pH no. 1 = 4, no. 2 = 10, and no. 3 = 10 for Pd(5 wt %)/C or pH no. 1 = 5, no. 2 = 8, and no. 3 = 10 for Pd(5 wt %)/C_f; $PdCl_2 + HNO_3$: pH no. 1 = 8, no. 2 = 10, and no. 3 = 10; $Pd(OAc)_2$ + HCl: pH no. 1 = 8, no. 2 = 8, and no. 3 = 10; and $PdCl_2$ + HCl: pH no. 1 = 8, no. 2 = 10, no. 3 = 10, where pH no. 1 = Pd solution stirred with aqueous suspension of carbon for 24 h, pH no. 2 = after addition of NaOH, and pH no. 3 = after chemical reduction. See Experimental Procedures for definition of *Y* and *S**. 1: From refs 30 and 31. 2: From ref 33.

with β_{OHn} as a global equilibrium stability constant, corresponding to

$$[Pd(H_2O)_4]^{2+} + nOH^- \rightleftharpoons [Pd(OH)_n(H_2O)_{4-n}]^{(2-n)+} + nH_2O \quad n = 1, 2, 3, 4 \quad (3)$$

$$[[Pd(Cl)_n(H_2O)_{4-n}]^{(2-n)+}] = \beta_{Cln}[Pd^{2+}][Cl^-]^n \quad n = 0, 1, 2, 3, 4 \quad (4)$$

with β_{Cln} as a global equilibrium stability constant, corresponding to

$$[Pd(H_2O)_4]^{2+} + nCl^- \rightleftharpoons [Pd(Cl)_n(H_2O)_{4-n}]^{(2-n)+} + nH_2O \quad n = 1, 2, 3, 4 \quad (5)$$

The speciation diagrams of the Pd(II) species as a function of pH are in general divided into three zones, differentiated by the charge of the Pd species present in solution. Acidic solutions contain Pd species that are positively charged, while basic solutions are constituted of negatively charged species. Between those two extremes, there is a pH range where the Pd(II) species are neutral. For a pCl value of 2.93, this pH range for neutrality is situated between pH 3.5 and 12, and it is reduced to pH 5−12 for a pCl of 0.92. As discussed previously,[35] the use of palladium acetate solubilized with nitric acid gives a pH range corresponding to neutral Pd species at pH values between 3 and 12.

3.4. Catalytic Properties of Pd/C Materials. By controlling the pH of the solutions during all synthetic steps, to keep the value within the maximum adsorption range, we have prepared a series of monometallic Pd(5 wt %)/C catalysts from both Pd precursors and both C_{SXPLUS} and functionalized carbon. In particular, the experimental pH values for the adsorption step of Pd on carbon were selected to correspond to the pH range where the highest Pd/C atomic intensity ratios were identified by XPS. All catalysts were tested in glyoxal oxidation (Figure 1). Figure 8 shows a comparison of the catalytic results obtained with these various materials. The first observation is that the catalysts are sensitive to the Pd precursor used. In each case, the materials prepared from $PdCl_2$ are less active than the corresponding ones prepared from $Pd(OAc)_2$. The effect of the solubilizing agent is less marked with, for example, the catalysts made from $Pd(OAc)_2$ and HCl or $Pd(OAc)_2$ and HNO_3 giving similar results, while in the case of $PdCl_2$, the use of HNO_3 always leads to poor performance. Moreover, the carbon support submitted to an oxidative treatment seems to have a slightly positive effect on the catalytic activity but mainly on the yield in formic acid, which is detrimental for the selectivity in glyoxalic acid. The Pd/C catalysts prepared here in an optimized fashion with SX PLUS carbon are more efficient than Pd/C catalysts reported so far for this reaction[30,31,33] and give results similar to those obtained with the most performant bimetallic Bi,Pb−Pd/C catalysts,[30,31] even though the selectivity is sometimes lower. In all cases, no Pd leaching was found in the reaction medium.

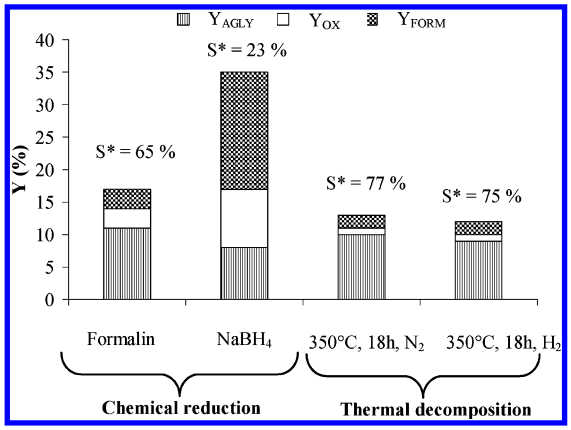

Figure 9. Catalytic results after 20 h for Pd(5 wt %)/C catalysts prepared from $Pd(OAc)_2 + HNO_3$ (pH no. 1 = 4, no. 2 = 5, and no. 3 = 9) and activated by four different methods. See Experimental Procedures for definition of *Y* and *S**.

The catalytic results for the four Pd/C samples, prepared from palladium acetate and nitric acid as a solubilizing agent, using the same pH values during all synthetic steps but activated by different methods are presented in Figure 9. The performance in terms of yield in glyoxalic acid after 20 h of reaction is not really influenced by the activating agent, but catalysts activated thermally seem to give a better selectivity in glyoxalic acid. In addition, the catalysts activated with sodium borohydride gave important amounts of formic and oxalic acids, thus decreasing the selectivity.

3.5. Characterization of Pd/C Materials. To verify if there is a correlation between the structure of the active phase and the catalytic activity of the Pd/C catalysts, these materials were characterized by a series of physicochemical techniques, whose results will be detailed here.

All catalysts were characterized by XPS to look for a possible link between the Pd/C surface atomic ratios and the catalytic activity. Two catalysts have been characterized by XPS at each step of their synthesis (Table 1). A first interesting observation was that the Pd/C ratios were high at each synthetic step (in comparison with the value calculated on the basis of the bulk composition (0.6)) and increased dramatically after addition of the base. Moreover, the heating step after addition of the reducing agent seems crucial for Pd reduction, and it is only after this step that the catalysts become active ($Y_{AGLY} \neq 0$). For all catalysts prepared in this work, it was found that the experimental atomic intensity ratios Pd/C, before and after catalytic tests, are superior to the values calculated on the basis of the bulk composition (Table 2), suggesting a good dispersion of the palladium on the support. Moreover, a majority of the

TABLE 1: XPS Results at Each Step of Synthesis of Pd/C Catalysts Prepared by (a) Using $Pd(OAc)_2$ Solubilized with HNO_3 (Activation at pH 11) and (b) Using $PdCl_2$ Solubilized with HCl (Activation at pH 11)

(a) synthetic step	Y_{AGLY} (%)	Pd/C (×100)[a]	oxidation state
(1) stirring of suspension of C and Pd solution (t = 18 h, pH = 6)	0	3.9	Pd(0) + Pd(II)
(2) addition of NaOH (t = 5 min, pH = 11)	0	8.1	Pd(0) + Pd(II)
(3) addition of formalin (t = 1 h, pH = 7)	0	2.4	Pd(0) + Pd(II)
(4) addition of formalin and heating at 80 °C (t = 1 h, pH = 5)	12	3.4	Pd(0)
(b) synthetic step	**Y_{AGLY} (%)**	**Pd/C (×100)[a]**	**oxidation state**
(1) stirring of suspension of C and Pd solution (t = 18 h, pH = 8)	0	2.7	Pd(0) + Pd(II)
(2) addition of NaOH (t = 5 min, pH = 11)	0	9.5	Pd(0) + Pd(II)
(3) addition of formalin (t = 1 h, pH = 11)	0	2.7	Pd(0) + Pd(II)
(4) addition of formalin and heating at 80 °C (t = 1 h, pH = 11)	9	5.5	Pd(0)

[a] Experimental (retrieved from XPS data analysis) Pd/C atomic intensity ratios, to be compared with value calculated from the bulk composition (0.6).

TABLE 2: XPS Results Before and After Catalytic Test (20 h) and CO Chemisorption Results for Pd (5 wt %)/C Catalysts

			Pd/C (×100)[a]			
			calcd	exptl		
catalyst[b]	preparation method	activation agent		before	after[c]	CO chemisorption[c]
Pd/C	$Pd(OAc)_2 + HNO_3$	formalin	0.6	4.0	3.9	17.1
Pd/C	$PdCl_2 + HNO_3$	formalin	0.6	1.2	1.5	0.5
Pd/C	$Pd(OAc)_2$ + HCl	formalin	0.6	2.7	2.6	n.d.
Pd/C	$PdCl_2$ + HCl	formalin	0.6	3.7	2.6	16.1
Pd/C_f	$Pd(OAc)_2 + HNO_3$[d]	formalin	0.6	4.6	4.6	12.1
Pd/C_f	$PdCl_2 + HNO_3$	formalin	0.6	1.3	1.3	1.9
Pd/C_f	$Pd(OAc)_2$ + HCl	formalin	0.6	3.9	3.9	16.2
Pd/C_f	$PdCl_2$ + HCl	formalin	0.6	2.6	2.6	21.5
Pd/C	deposition[e]	N_2	0.6	1.2	1.1	1.3
Pd/C	commercial[f]	unknown	0.6	2.2	n.d.	13.8
Bi-Pd/C	deposition[e]	N_2	0.4	0.3	0.4	n.d.
Pd/C	$Pd(OAc)_2 + HNO_3$	formalin	0.6	2.8	2.2	16.5
Pd/C	$Pd(OAc)_2 + HNO_3$	$NaBH_4$	0.6	4.2	3.6	7.8
Pd/C	$Pd(OAc)_2 + HNO_3$	N_2	0.6	3.9	2.6	7.3
Pd/C	$Pd(OAc)_2 + HNO_3$	H_2	0.6	3.6	2.8	10.1

[a] Pd/C atomic intensity ratios: calcd = values calculated from the bulk composition; exptl = experimental values retrieved from XPS data analysis; before = before catalytic test; and after = after one use during 20 h in the catalytic oxidation of glyoxal. [b] Sample $Pd(OAc)_2 + HNO_3$: pH no. 1 = 4, no. 2 = 10, and no. 3 = 10. Sample $PdCl_2 + HNO_3$: pH no. 1 = 8, no. 2 = 10, and no. 3 = 10. Sample $Pd(OAc)_2$ + HCl: pH no. 1 = 8, no. 2 = 8, and no. 3 = 10. Sample $PdCl_2$ + HCl: pH no. 1 = 8, no. 2 = 10, and no. 3 = 10, where pH no. 1 = Pd solution stirred with aqueous suspension of carbon for 24 h, pH no. 2 = after addition of NaOH, and pH no. 3 = after chemical reduction. C_f = functionalized carbon. [c] n.d. = not determined. [d] pH no. 1 = 5, no. 2 = 8, and no. 3 = 10. [e] From refs 30 and 31 and after 24 h of catalytic test. [f] From ref 33.

Pd was present as metallic palladium on the surface. The degree of reduction was evaluated by decomposition of the Pd 3d photopeaks as exemplified in Figure 10. It was found that the catalysts were inactive if the Pd was not totally reduced. Catalysts prepared with $PdCl_2$ as the Pd precursor and nitric acid as the solubilizing agent display the smallest experimental Pd/C atomic intensity ratios. The comparison of XPS data before and after testing shows that the Pd/C surface ratios have not been visibly modified after use. The four Pd/C catalysts prepared using the same synthetic conditions, but with different reducing agents, were also characterized by XPS. Again, the experimental Pd/C ratios are very high (Table 2), especially for the catalyst activated with sodium borohydride.

The palladium dispersion at the surface of the catalysts was obtained by CO chemisorption (Table 2). This indicates that, when the percentage of active metallic atoms accessible to the reactants is high, the catalytic activity of the materials is important.

Four representative Pd/C catalysts were examined by SEM and TEM (Figures 11 and 12). The SEM images obtained for materials prepared with $Pd(OAc)_2$ and HNO_3 (Figure 11a) and $PdCl_2$ and HCl (Figure 11c) show a homogeneous distribution of small Pd particles (bright dots, ~10−15 nm in size), while electron micrographs for a Pd/C catalyst prepared with $PdCl_2$ and HNO_3 (Figure 11b) show an agglomeration of metallic particles on the carbon surface, giving particle sizes of up to 400 nm. This was confirmed by TEM (see, i.e., Figure 12a, which is the same sample as in Figure 11a and shows very small particles). The catalyst activated with sodium borohydride was also characterized by TEM (Figure 12b) and the electron micrographs revealed a homogeneous distribution of very small particles (<10 nm) on the surface.

4. Discussion

4.1. Carbon PZC and IEP. As already mentioned in the Introduction, the surface of activated carbons is invariably associated with appreciable amounts of heteroatoms such as oxygen and hydrogen, having a great effect on the adsorption properties of carbonaceous supports. Consequently, both negatively and positively charged surface sites exist in aqueous solution, depending on the pH, and rely on two parameters: the PZC and the IEP, often unfortunately confused. Although some determination techniques for these two factors are available, their limitations are repeatedly cited. For example, Regalbuto and Park disliked the mass titration method, which is widely used to determine carbon PZC and suggested an extension of the modeling of surface charges for PZC measurement.[38] That is why we have used both methods (mass titration or a modified version of Regalbuto) to determine PZC values for the two carbons used in this study (C and C_f). A first observation is

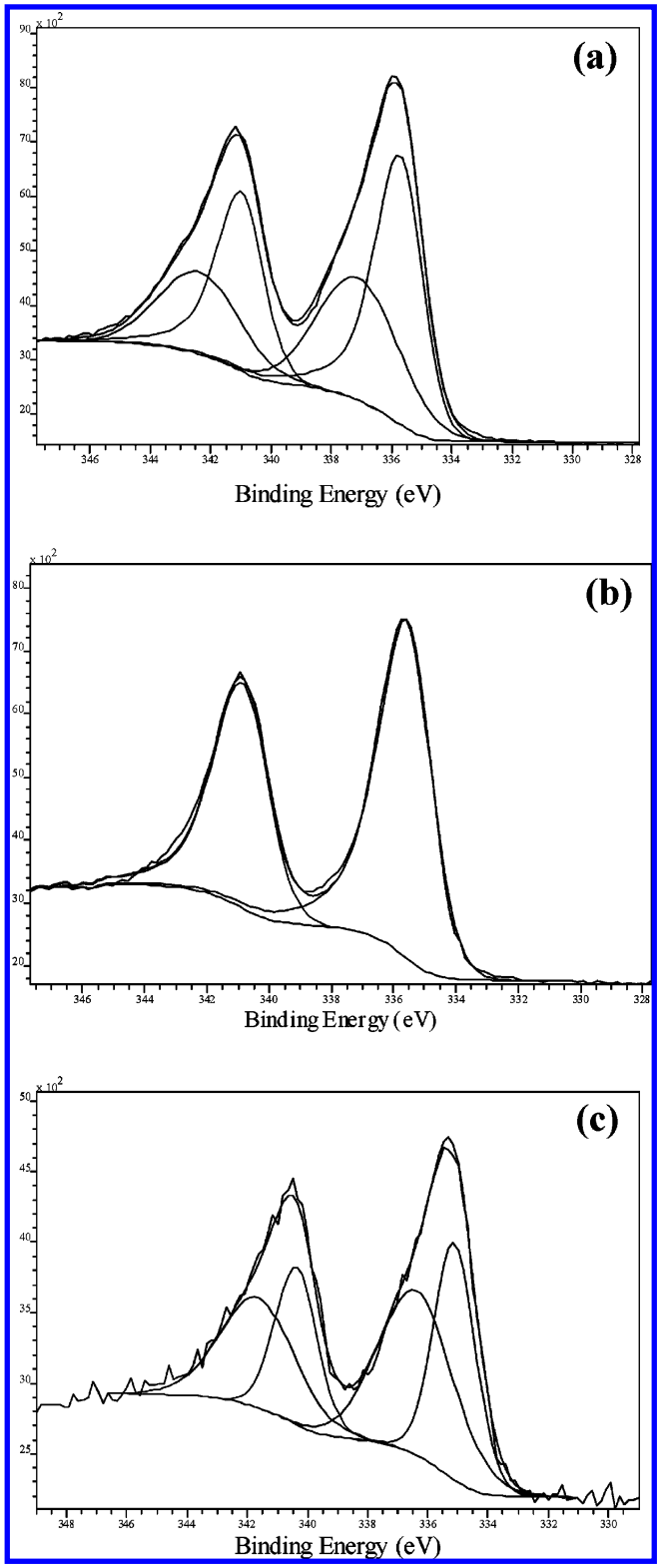

Figure 10. Example of XPS results in the Pd3d region for a (a) not completely reduced, (b) reduced catalyst, and the (c) Pd/C commercial catalyst.[33]

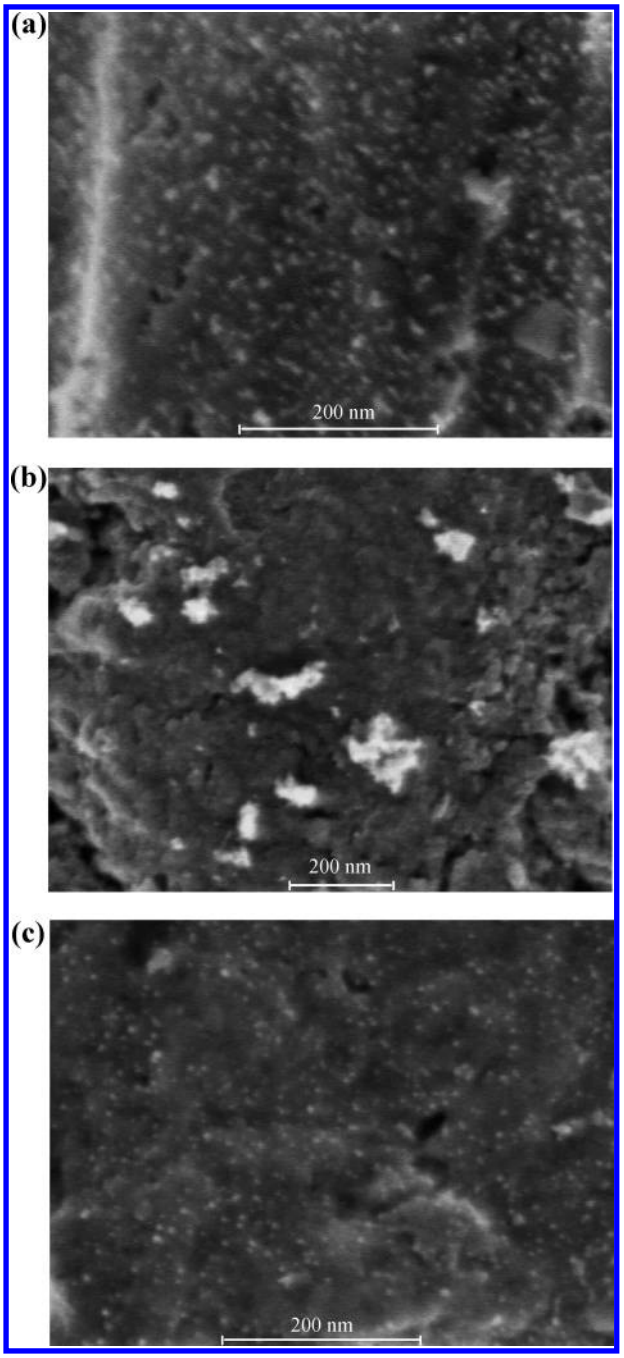

Figure 11. SEM images obtained for representative catalysts prepared on SX PLUS carbon and activated by formalin: (a) $Pd(OAc)_2 + HNO_3$ (×200 000), (b) $PdCl_2 + HNO_3$ (×100 000), and (c) $PdCl_2 + HCl$ (×200 000).

that these two different experimental procedures give identical PZC values for each of the two carbon samples. As pointed out by Regalbuto, the limitation of the mass titration method appears when the starting solution is extremely acidic or basic. For example, when using 1.3 as a starting pH value (Figure 2b), the curve never tends toward a plateau, even for high mass loading. We have also used electrophoretic mobility measurements to determine the respective IEP values for both supports.

Knowing these two parameters (PZC and IEP) permits us to state the following: (i) below the IEP value, the surface of the carbon support is mainly positively charged and (ii) at a pH superior to the PZC, the carbon surface is covered by deprotonated acidic groups and hence is mainly negatively charged. Between the IEP and the PZC, the situation is subject to debate. According to Radovic et al. and others,[42−44] the IEP is only representative of the external surface charges of the carbon particles in solution, while the PZC is defined by referring to the net total (external and internal) surface charge of the particles. Hence, the difference between PZC and IEP values

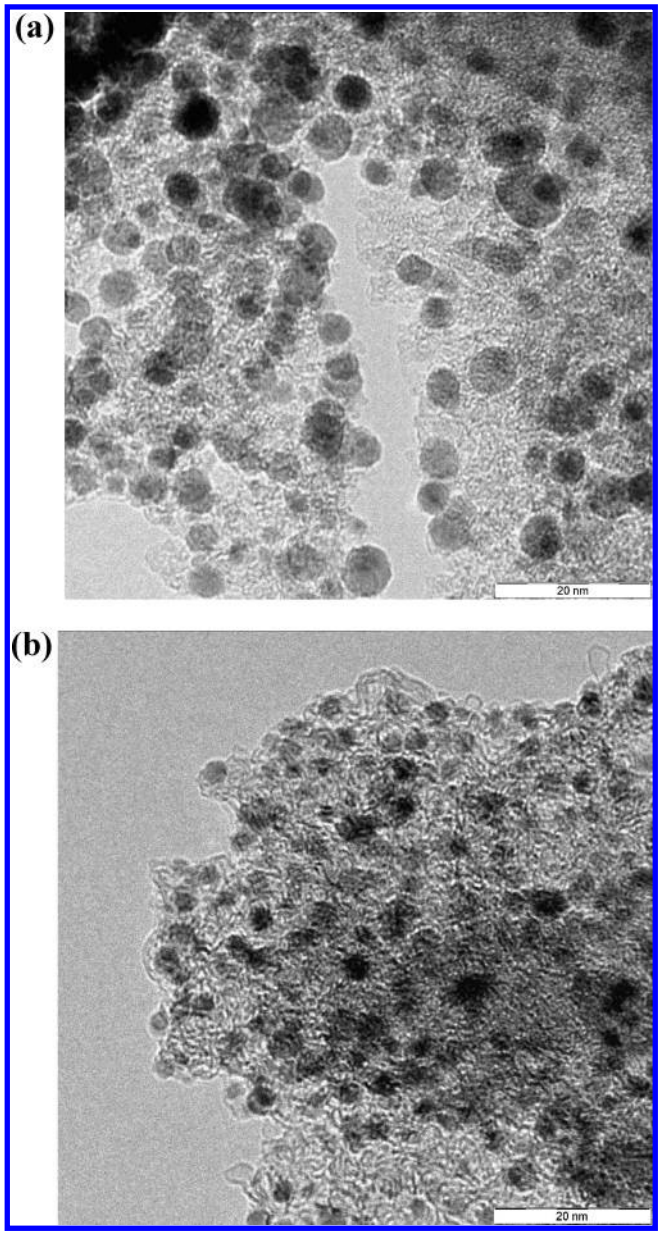

Figure 12. TEM images obtained for representative catalysts prepared on SX PLUS carbon: (a) catalyst prepared from $Pd(OAc)_2 + HNO_3$ and activated by formalin (same sample as Figure 11a) and (b) catalyst prepared from $Pd(OAc)_2 + HNO_3$ and activated with $NaBH_4$.

could be interpreted as a measure of the charge distribution in porous carbons. Values greater than zero indicate more negatively charged external than internal particle surfaces, and values close to zero correspond to a more homogeneous distribution of the surface charges.

Values of PZC and IEP for different activated carbons (with similar specific surface areas as those of our samples), as reported by various authors, are listed in Table 3. The literature PZC values are similar to our data or are in the same pH range for both carbons (8.1 and 2.5, respectively, for an activated carbon SX-ULTRA and an activated carbon CA1 oxidized with concentrated phosphoric acid[16] or 2.8 for an activated carbon treated with HNO_3 (70% vol) for 30 min at a boiling temperature[45]). The IEP values obtained by us are also in agreement with the literature data.

4.2. Adsorption Mode of Pd Species on Carbon Supports. To gain a better understanding of the phenomena involved, which lead to a better adsorption of the Pd species on the support within some specific pH windows, the results of PZC and IEP determination and Pd(II) speciation were compared with the adsorption curves. More specifically, to observe the influence of the Pd species charge and the IEP and PZC values of the support on Pd adsorption, we have superimposed the Pd adsorption curves with the corresponding speciation diagrams for Pd(II) as a function of pH (Figures 13 and 14). In each case, the maximum adsorption range corresponds to the window of existence of a neutral Pd species such as $[Pd(OH)_2(H_2O)_2]$, while the carbon surface is either positively or negatively charged (or even presents a net surface charge equal to zero). Above or below the range for maximum adsorption, in each case, a charge mismatch appears, leading to repulsive electrostatic interactions between the Pd species and the carbon surface: at low pH, both the Pd(II) species and the support surface are positively charged, while at high pH, both of them are negatively charged. These trends are very clear for the pristine C_{SXPLUS} (C, see Figure 13) but perhaps not as valid in the case of the functionalized carbon (C_f, see Figure 14).

The fact that maximum adsorption occurs in each case when the Pd species are neutral does not allow us to use a simple electrostatic model to explain the adsorption of the metallic precursors onto the carbon surface from aqueous solution. Electrostatic interactions may be involved when considering the zones of weak interaction, as mentioned previously, by considering repulsive forces between species bearing the same charge. However, in the maximum adsorption range, the Pd species are neutral, and the carbon surface is slowly obtaining its negative charge as the pH increases. This might suggest that palladium adsorption in aqueous solution involves ligand exchanges with surface functions that are the subject of protonation/deprotonation as a function of the pH or that neutral Pd species settle on the C surface with a localized precipitation phenomenon. The fact that Pd adsorption on functionalized carbon (C_f) seems to present in some cases wider pH windows than for the case of Pd adsorption on SX PLUS carbon (C) could be explained by the larger amount of oxygenated surface groups on functionalized carbon. Indeed, it is known that activated carbons are hydrophobic in general and are associated with small amounts of oxygenated surface groups. Such activated carbons are more suitable for the adsorption of neutral compounds, and they show little affinity for ionic complexes. However, increasing the amount of carbon−oxygen surface groups, acidic in character, such as carboxylic acid and lactones, makes the surface hydrophilic and may enhance the adsorption of positively charged species from the aqueous phase, and this enhanced ability may be attributed to their ion exchange properties.[46] Moreover, we knew that the carbon oxidation treatment used in this work increased the number of oxygenated surface functions, particularly carboxylic functions,[36,47] giving a partial explanation for the adsorption window extension in the case of the functionalized carbon. Even if not fully explained, the identification of a maximum adsorption range for Pd on carbon allows us to prepare active catalysts in optimized conditions.

These results do not agree fully with the interpretation given by Regalbuto et al.,[16,18] who used a purely electrostatic model for rationalization of Pt adsorption onto oxide surfaces and carbonaceous supports. This electrostatic adsorption mechanism assumes that below the PZC, the hydroxyl groups covering the surface become protonated, and the surface can adsorb anionic metal complexes such as hexachloroplatinate(IV), while above the PZC, the hydroxyl groups become negatively charged, and cations such as tetraammine platinum(II) can be strongly

TABLE 3: Summary of Some Characteristics of Carbon Supports Used in This Work and from the Literature

type of carbon	surface area (m^2/g)	total acidity (mmol/100 g of C)[a]	PZC value	IEP value[a]
	This work			
C (SX PLUS)	922[b]	32.0[b]	8.5	3.5
C_f (functionalized SX PLUS)	756[b]	325.6[b]	2.3	<2
	Literature			
Norit SX-Ultra[c]	1200	n.d.	8.1	n.d.
Norit CA1[c]	1400	n.d.	2.5	n.d.
Norit C treated with HNO_3 (70 vol %) for 30 min[d]	1240	n.d.	2.8	1.4

[a] n.d. = not determined. [b] From ref 36. [c] From ref 16. [d] From ref 45.

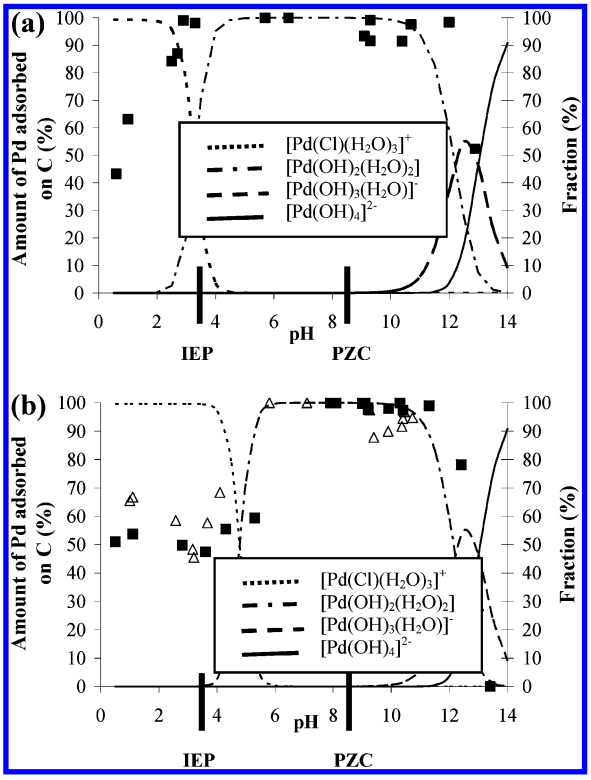

Figure 13. Superimposition of Pd adsorption curves on C_{SXPLUS} with the Pd speciation diagram as a function of pH for (a) pCl value of 2.93: $PdCl_2 + HNO_3$ and (b) pCl value of 0.92: ■ $Pd(OAc)_2$ + HCl and △ $PdCl_2$ + HCl.

absorbed. However, EXAFS studies carried out by Regalbuto's group have revealed the exchange of Cl ligands for O ligands during adsorption, which suggests a more sophisticated adsorption mechanism than a simple electrostatic model. A disagreement with the theory of Regalbuto's group is that, according to them, maximum adsorption is realized between a positively charged surface and negatively charged precursors or between a negatively charged surface and positively charged precursors. In our case, the range of maximum Pd adsorption contains pH values corresponding to the PZC, which, according to Regalbuto, should lead to minimal adsorption, as it involves only neutral partners. Radovic et al.[42] have also concluded that maximum catalyst dispersion is favored when the entire carbon surface is chemically accessible (i.e., when there is electrostatic attraction between a positively charged surface (below pH_{IEP}) and the catalyst precursor anions or between a negatively charged surface (above pH_{IEP}) and the catalyst precursor cations). It follows that the pH of the precursor solution determines the nature as well as the amount of charged surface sites and, thus, the number of counterions that can be adsorbed.

Even the experiments carried out to understand the role of ions such as Na^+ and Cl^- on the Pd dispersion demonstrate that the maximum adsorption range corresponds to the window

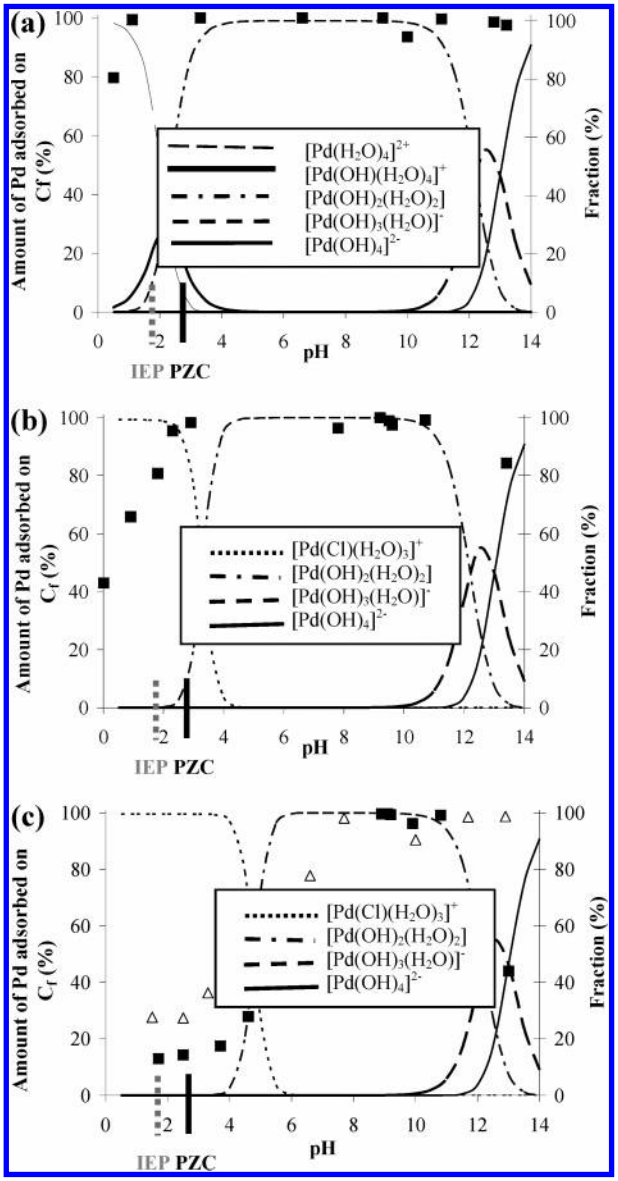

Figure 14. Superimposition of Pd adsorption curves on functionalized carbon with the Pd speciation diagram as a function of pH for (a) $Pd(OAc)_2 + HNO_3$, (b) pCl value of 2.93: $PdCl_2 + HNO_3$, and (c) pCl value of 0.92: ■ $Pd(OAc)_2$ + HCl and Δ $PdCl_2$ + HCl.

of existence of neutral Pd species. Indeed, by taking into consideration the actual chloride concentration in these experiments, the first three pH values (8.5, 9.6, and 10.7, where adsorption occurs) are in a pH range corresponding to neutral Pd species, while a pH value of 4.9 (where adsorption is not optimal), giving 0.6 as the pCl value, corresponds to a positively charged Pd species. Regalbuto has attributed a deleterious effect of high ionic strength on metallic uptake,[18] but this effect is not observed here.

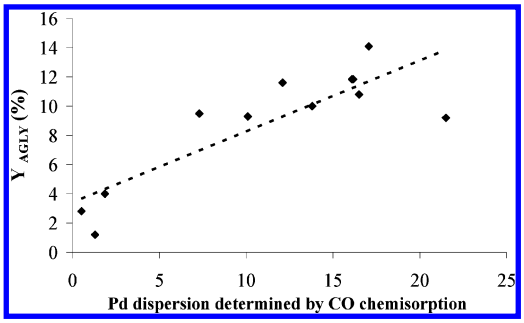

Figure 15. Evolution of the yield in glyoxalic acid after 20 h as a function of palladium dispersion (from CO chemisorption).

4.3. Relationship between Catalytic Properties and Physicochemical Characterization of Pd Catalysts. First, XPS measurements have shown that the catalysts prepared in this work present very high experimental Pd/C ratios, suggesting a good dispersion of Pd on the support. Catalysts presenting the smallest experimental Pd/C atomic intensity ratios give a lower catalytic activity. However, no quantitative correlation appears between the values of Pd/C ratios measured by XPS and the values of yields in glyoxalic acid. The catalysts were inactive if the Pd was not totally reduced, implying that Pd(0) is the active phase. These observations suggest that high activities are related, on the one hand, to high Pd dispersions and, on the other hand, to an important degree of Pd reduction. This also explains why the commercial catalyst is less active, even though characterized by a high dispersion: the XPS photopeaks for Pd clearly show the presence of a mixture of Pd(0) and Pd(II) (Figure 10c). Second, CO chemisorption results show that the catalytic activity of the materials is important when the percentage of active metallic atoms accessible to the reactants is high. In this case, a linear correlation between palladium dispersion and yield in glyoxalic acid after 20 h exists (Figure 15). This shows again that the active species is the reduced Pd(0) and that a simple increase of the Pd dispersion improves the activity of the catalysts. Third, the SEM and TEM images indicate that the inactive catalysts display an agglomeration of large particles (up to 400 nm) on the carbon surface, while the active materials show a homogeneous distribution of small Pd particles on the support. This is in line with the values of dispersion obtained by CO chemisorption. Moreover, the electron micrographs of the catalyst activated with sodium borohydride show a homogeneous distribution of very small particles (<10 nm) on the surface. This observation could explain the production of important amounts of formic and oxalic acids, as discussed previously.[33]

This allows us to evidence relationships between the structure of the catalysts and their activity in glyoxalic acid. The synthetic method used in this work gives active catalysts, with metallic palladium as the active species, and high surface Pd/C ratios, correlated to high dispersion measured by CO chemisorption and small particles sizes observed by SEM/TEM. These results confirm that a high Pd dispersion in the form of small particles can be obtained by using the controlled preparation method described here. The possible explanation for this significant catalytic activity is the maximization of the interactions between the Pd precursor and the support in aqueous solution during impregnation, which leads to a homogeneous distribution of small metallic particles on the support after activation. This can be rationalized by taking into account the influence of the nature of metal species present in solution and in particular their charge in comparison to the C surface charge, which both vary as a function of pH.

5. Conclusion

In this work, we have shown that Pd/C catalysts prepared in an optimized fashion, by controlled adsorption, are very active in liquid-phase selective oxidation. The optimization of the preparation method has involved (i) determining the PZC and the IEP of the carbon support, (ii) identifying the pH range where maximum adsorption of Pd on C occurs, for the two precursors envisaged ($Pd(OAc)_2$ and $PdCl_2$), and (iii) establishing the speciation diagrams for the various possible Pd(II) species in solution as a function of pH and pCl. Monometallic Pd/C catalysts were then prepared by fixing the pH of the synthetic medium within the maximum adsorption range. The obtained catalysts were very active for the selective oxidation of glyoxal into glyoxalic acid, and more so than previously described Pd/C materials, to give performances similar to that of bimetallic Pd−M/C (M = promoter element) catalysts. The Pd/C catalysts were characterized by XPS, SEM, TEM, and CO chemisorption. The active materials were characterized by high Pd/C surface ratios and by an important degree of Pd reduction. Moreover, the high activity was connected to (i) high Pd dispersion measured by CO chemisorption and (ii) very small particles homogeneously dispersed on the C support observed by SEM/TEM. These observations were true whatever the activating agent used, with the exception of $NaBH_4$, which gave a decrease in selectivity and remained valid after 20 h of catalytic testing. These optimized catalytic results obtained with monometallic materials allow us to envision the addition of a promoting element in a similar manner to increase further the activity and selectivity.

Acknowledgment. The authors greatly acknowledge financial support from the Belgian National Fund for Scientific Research (FNRS, Brussels) and the firm Norit for supplying the carbon support. We are also grateful to Prof. E. M. Gaigneaux for access to XPS, Prof. P. Rouxhet for access to electrophoretic potential measurements, and M. Genet, Y. Adriaensen, and J.-F. Statsijns for useful discussions and technical assistance.

References and Notes

(1) Blaser, H.-U.; Indolese, A.; Schnyder, A.; Steiner, H.; Studer, M. *J. Mol. Catal. A: Chem.* **2001**, *173*, 3−18.
(2) Vinke, P.; de Wit, D.; de Goede, A. T. J. W.; van Bekkum, H. *Stud. Surf. Sci. Catal.* **1992**, *72*, 1−18.
(3) van Bekkum, H. *Stud. Surf. Sci. Catal.* **1999**, *121*, 117−126.
(4) Mallat, T.; Baiker, A. *Catal. Today* **1994**, *19*, 247−284.
(5) Besson, M.; Gallezot, P. *Catal. Today* **2000**, *57*, 127−141.
(6) Besson, M.; Gallezot, P. *Fine Chemicals through Heterogeneous Catalysis*; VCH: Weinheim, 2001; Ch. 9; pp 491−506.
(7) Toebes, M. L.; van Dillen, J. A.; de Jong, K. P. *J. Mol. Catal. A: Chem.* **2001**, *173*, 75−98.
(8) Farkas, G.; Hegedus, L.; Tungler, A.; Mathe, T.; Figueiredo, J. L.; Freitas, M. *J. Mol. Catal. A: Chem.* **2000**, *153*, 215−219.
(9) Gurrath, M.; Kuretzky, T.; Boehm, H. P.; Okhlopkova, L. B.; Lisitsyn, A. S.; Likholobov, V. A. *Carbon* **2000**, *38*, 1241−1255.
(10) Heal, G. R.; Mkayula, L. L. *Carbon* **1988**, *26*, 815−823.
(11) Yang, Y.; Zhou, Y.; Cha, C.; Carroll, W. M. *Electrochim. Acta* **1993**, *38*, 2333−2341.
(12) Simonov, P. A.; Romanenko, A. V.; Prosvirin, I. P.; Moroz, E. M.; Boronin, A. I.; Chuvilin, A. L.; Likholobov, V. A. *Carbon* **1997**, *35*, 73−82.
(13) Benedetti, A.; Bertoldo, L.; Canton, P.; Goerigk, G.; Pinna, F.; Riello, P.; Polizzi, S. *Catal. Today* **1999**, *49*, 485−489.
(14) Albers, P.; Burmeister, R.; Seibold, K.; Prescher, G.; Parker, S. F.; Ross, D. K. *J. Catal.* **1999**, *181*, 145−154.
(15) Auer, E.; Freund, A.; Pietsch, J.; Tacke, T. *Appl. Catal. A* **1998**, *173*, 259−271.
(16) Hao, X.; Quach, L.; Korah, J.; Spieker, W. A.; Regalbuto, J. R. *J. Mol. Catal. A: Chem.* **2004**, *219*, 97−107.
(17) Jolivet, J.-P. *De la Solution à l'Oxyde*; InterEditions/CNRS Editions: Paris, 1994; Ch. 7; pp 281−283.

(18) Regalbuto, R. *Surface and Nanomolecular Catalysis*; CRC Press: Boca Raton, FL, 2006; Ch. 6; pp 161−193.
(19) Parks, G. A. *Chem. Rev.* **1965**, *65*, 177−198.
(20) Mattioda, G.; Christidis, Y. *Ullmann's Encyclopedia of Industrial Chemistry*, 5th Ed.; VCH: Weinheim, 1989; Ch. A12; pp 495−497.
(21) Li, K.; Frost, J. W. *J. Am. Chem. Soc.* **1998**, *120*, 10545−10546.
(22) Hoefnagel, A. J.; van Bekkum, H.; Peters, J. A. *J. Org. Chem.* **1992**, *57*, 3916−3921.
(23) Meester, W. J. N.; van Maarseveen, J. H.; Schoemaker, H. E.; Hiemstra, H.; Rutjes, F. P. J. T. *Eur. J. Org. Chem.* **2003**, 2519−2529.
(24) Isobe, K.; Nishise, H. *J. Biotechnol.* **1999**, *75*, 265−271.
(25) Gavagan, J. E.; Fager, S. K.; Seip, J. E.; Payne, M. S.; Anton, D. L.; DiCosimo, R. *J. Org. Chem.* **1995**, *60*, 3957−3963.
(26) Yadav, G. D.; Gupta, V. R. *Process Biochem. (Oxford)* **2000**, *36*, 73−78.
(27) Pierre, G.; El Kordi, M.; Cauquis, G. *Electrochim. Acta* **1985**, *30*, 1227−1230.
(28) Scott, K. *Electrochim. Acta* **1991**, *36*, 1447−1452.
(29) Gallezot, P.; de Mésantourne, R.; Christidis, Y.; Mattioda, G.; Schouteeten, A. *J. Catal.* **1992**, *133*, 479−485.
(30) Alardin, F.; Delmon, B.; Ruiz, P.; Devillers, M. *Catal. Today* **2000**, *61*, 255−262.
(31) Alardin, F.; Ruiz, P.; Delmon, B.; Ruiz, P.; Devillers, M. *Appl. Catal., A* **2001**, *215*, 125−136.
(32) Alardin, F.; Wullens, H.; Hermans, S.; Devillers, M. *J. Mol. Catal. A: Chem.* **2005**, *225*, 79−89.
(33) Deffernez, A.; Hermans, S.; Devillers, M. *Appl. Catal., A* **2005**, *282*, 303−313.
(34) Hermans, S.; Devillers, M. *Catal. Lett.* **2005**, *99*, 55−64.
(35) Deffernez, A.; Hermans, S.; Devillers, M. *Stud. Surf. Sci. Catal.* **2006**, *162*, 79−86.
(36) Hermans, S.; Diverchy, C.; Demoulin, O.; Dubois, V.; Gaigneaux, E. M.; Devillers, M. *J. Catal.* **2006**, *243*, 239−251.
(37) Noh, J. S.; Schwarz, J. A. *J. Colloid Interface Sci.* **1989**, *130*, 157−164.
(38) Park, J.; Regalbuto, J. R. *J. Colloid Interface Sci.* **1995**, *175*, 239−252.
(39) Sillen, L. G. *Stability Constants of Metal−Ion Complexes, Section I*; The Chemical Society: London, 1964; p 57.
(40) Sillen, L. G. *Stability Constants of Metal−Ion Complexes, Section I*; The Chemical Society: London, 1964; p 283.
(41) Wood, S. A. *Geochim. Cosmochim. Acta* **1991**, *55*, 1759−1767.
(42) Leon y Leon, C. A.; Solar, J. M.; Calemna, V.; Radovic, L. R. *Carbon* **1992**, *30*, 797−811.
(43) Corapcioglu, M. O.; Huang, C. P. *Carbon* **1987**, *25*, 569−578.
(44) Newcombe, G.; Hayes, R.; Drikas, M. *Colloids Surf., A* **1993**, *78*, 65−71.
(45) Menendez, J. A.; Illan-Gomez, M. J.; Leon y Leon, C. A.; Radovic, L. R. *Carbon* **1995**, *33*, 1655−1659.
(46) Bansal, R. C.; Goyal, M. *Activated Carbon Adsorption*; CRC Press: Boca Raton, FL, 2006; Ch. 6; pp 297−371.
(47) Diverchy, C.; Hermans, S.; Dubois, V.; Devillers, M. *Stud. Surf. Sci. Catal.* **2006**, *162*, 569−576.